MODELING PITTING AND CORROSION PHENOMENA BY EDDY-CURRENT VOLUME-INTEGRAL EQUATIONS[1]

Harold A. Sabbagh, Elias H. Sabbagh, R. Kim Murphy
Victor Technologies, LLC, PO Box 7706, Bloomington, IN 47407-7706 USA
Jimmy Ie, Purdue University, West Lafayette, IN 47907-1285 USA

We apply **VIC-3D©**, a proprietary volume-integral code for eddy-current nondestructive evaluation (NDE), to the problem of simulating the response of a probe to pitting. We utilize the solid-modeling library in **VIC-3D©** to simulate pitting found in heat-exchanger tubes by means of three-dimensional ellipsoids. The same model can be applied to pitting and corrosion phenomena in aerospace structures, as well. We demonstrate the forward problem of determining the response of the probe to a known pit, and then the inverse problem, in which a pit has been manufactured in a stainless-steel substrate, and multifrequency data are obtained by means of a Hewlett-Packard network analyzer. The resulting impedance data are inverted by using a nonlinear least-squares estimator that is a part of the post-processing capability of **VIC-3D©**. The result of the inversion is an estimate of the size of the pit, given by the lengths of the three semi-axes of the approximating ellipsoid, and the location of the pit.

[1] Presented at the 16th World Conference on Nondestructive Testing, Montreal, Thursday, 02SEP04

An Ellipsoidal Model for Pits. In this note we describe our initial results in modeling pits as three-dimensional semi-ellipsoids that originate in the inner-radius of tube walls. Figure 1 illustrates the model, together with its three defining parameters, the semi-axes, A, B, and C.

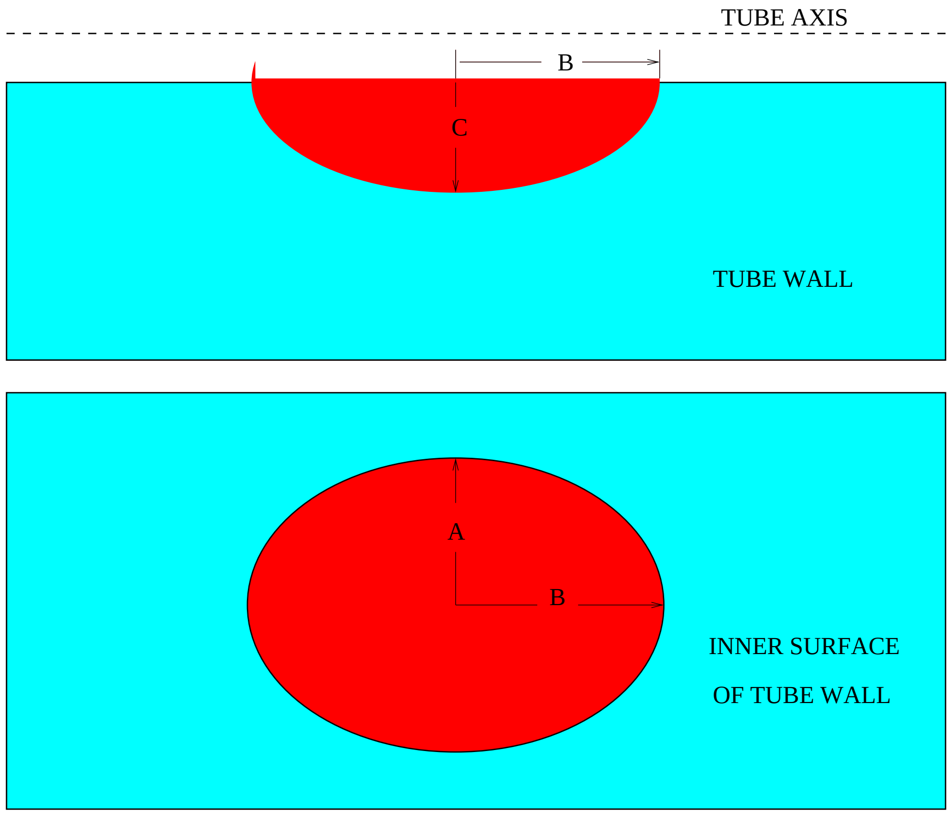

Figure 1: Illustrating a model of pits as three-dimensional semi-ellipsoids that originate in the inner-radius of a tube wall. The ellipsoid is defined by its three semi-axes, A, B, and C.

By modeling the pit in this manner, we hope to simplify the 'inverse problem,' which is to determine the size of the pit (especially its depth) from measured data. In this case, we hope to determine the three semi-axes, thereby solving the inverse problem. Clearly, C determines the depth of the pit.

The idea of representing pits as semi-ellipsoids was motivated partly by photomicrographs of actual pits that appear in certain heat-exchanger tubes in nuclear power plants. Furthermore, these photomicrographs gave us insight into the sizes of typical pits, which was then translated into values of A, B, and C for typical pits. Indeed, from these photomicrographs we see that the pits appear to be circular, when looking into the inner surface of the tube, with a nominal radius of 0.0625 inch. Hence, we model these pits by setting A and B equal to 0.0625. We then choose C to be equal to the difference between 0.049 inch (the nominal wall thickness of the heat-exchanger tube) and the minimum measured wall thickness, as given in the photomicrographs.

Computing Impedance Signatures With VIC-3D©. The first calculations that we made using **VIC-3D©** were to determine the impedance signature versus depth for the various pits, whose micrographs were described above. These pits are labeled 'Indication No. 3-9.' In all cases, we fixed A and B to be equal to 0.0625 inch, as explained above. The results are shown in Figure 2.

Clearly, the depth, as measured by the semi-axis, C, is quite distinguishable in these curves.

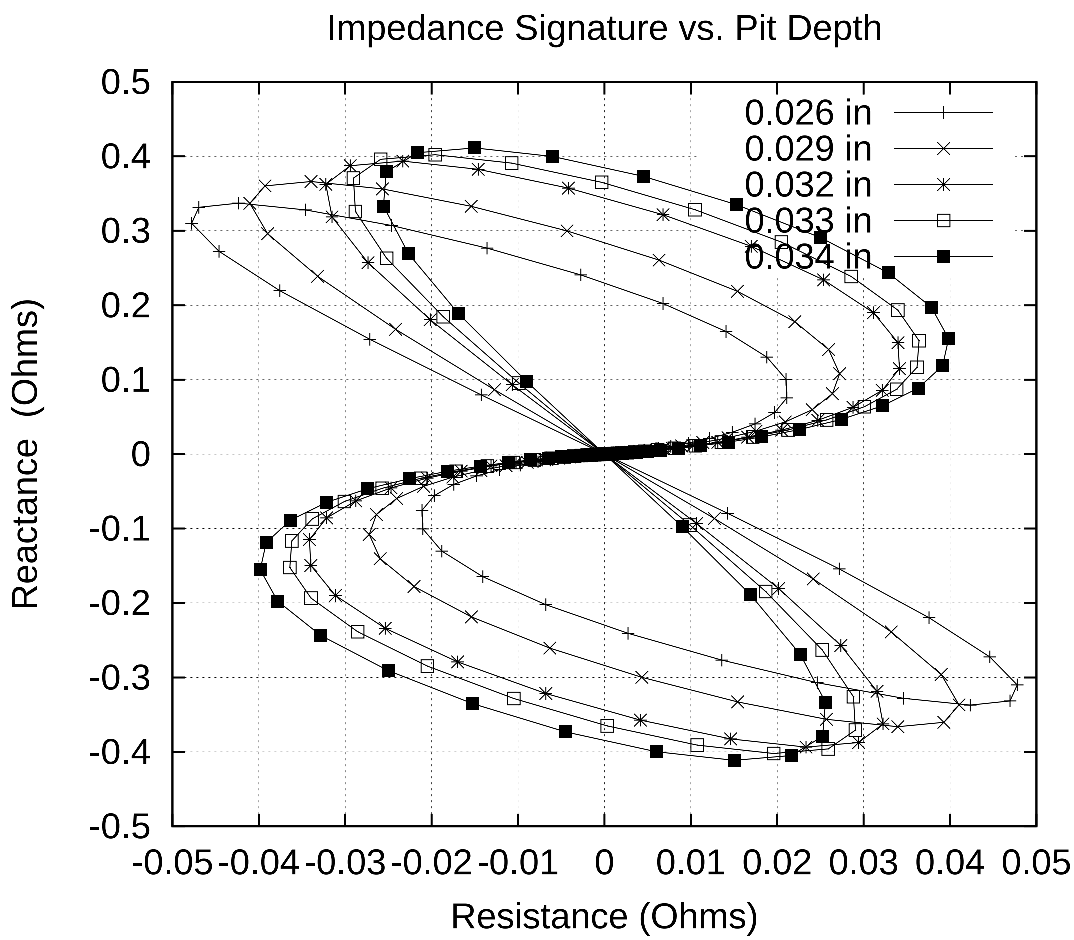

Figure 2: Impedance signature versus pit depth for the five pits labeled 'Indication No. 3, 4, 5, 7, 9.' The semi-axes A and B are set equal to 0.0625 inch for all five, and C is equal to the pit depth.

In carrying out the model calculations in this report, we assume that the tube is made of 90-10 Copper-Nickel, whose electrical conductivity is $\sigma = 5.277 \times 10^6$ S/m (9.1% IACS), and is nonmagnetic. The outer diameter of the tube is 0.75 inch, and the nominal wall thickness is 0.049 inch.

The coil parameters are given in the table

Coil Spacing	0.060 inch
Coil Height	0.055
Coil Width	0.060
Coil OD	0.576
Coil ID	0.466
Coil Turns	156

,

and the frequency of operation is assumed to be 70kHz.

It would be quite easy to model pits filled with corrosion deposits, whether conducting or magnetic (or both), with **VIC-3D©** but the observations quoted in data available to us are that the deposits consisted of cuprous oxide and copper carbonate, which are nonconducting. Hence, there was no need to include them in the model.

The Inversion Problem. Now we consider the inversion problem in detail. We took the model data of Figure 2 and used them to simulate measured impedance data, which were then submitted to the nonlinear least-squares estimator, NLSE, that is a part of the postprocessing capability of **VIC-3D©**. The output of NLSE is an estimate of the semi-axes, A, B, and C of the ellipsoidal pit, as displayed in Table 1.

Indication	Original Model Data (in)	Reconstructed (Inverted) Data (in)
No. 3	A=0.0625, B=0.0625, C=0.026	A=0.0643, B=0.0634, C=0.0263
No. 4	A=0.0625, B=0.0625, C=0.034	A=0.0644, B=0.0639, C=0.0325
No. 5	A=0.0625, B=0.0625, C=0.029	A=0.0645, B=0.0637, C=0.0285
No. 7	A=0.0625, B=0.0625, C=0.033	A=0.0645, B=0.0639, C=0.0316
No. 8	A=0.0500, B=0.0700, C=0.034	A=0.0550, B=0.0686, C=0.0328
No. 9	A=0.0625, B=0.0625, C=0.032	A=0.0645, B=0.0639, C=0.0309

Table 1: Estimate of A, B, and C for the semi-ellipsoidal representation of the pits labeled Indication No. 3-9.

Indication No. 8 was handled differently from the others. Because the X-Y cross-section of this pit was not circular, we found it more reliable to acquire data for it using a surface pancake probe scanned in a two-dimensional raster pattern. These data were then submitted to the estimator exactly as were the other five.

The results displayed in Table 1 indicate that the alogrithm for nonlinear estimation is reliable and robust. The maximum error occurs in A for Indication No. 8, and is only 10%, which is quite tolerable for this dimension (the width of the pit). The important point to be made from this study is the reliability in reconstructing C, the semi-axis that determines the depth of the pit. Indeed, the results of the algorithm indicate that the computation is more sensitive to depth then to the lateral dimensions, which is exactly what we're looking for!

Inversion of a Complex Pit. Figure 3 illustrates a complex pit, comprising three intersecting semi-ellipsoids. The A and B semi-axes are 0.0625 inches, as before, and the C semi-axes are 0.029, 0.026 and 0.034 inches. In this exercise, we assume that the A and B semi-axes are known, and the job is to determine the profile-in-depth of the pit, that is, to determine the three C-axes. The input data to NLSE at six frequencies, 10kHz, 20kHz, 40kHz, 70kHz, 200kHz, and 700kHz are shown in Figure 4. The results of applying NLSE at these frequencies, are shown in Table 2. The interesting result is the average over the six frequencies. Clearly, the reconstruction in depth is robust, especially when frequency scanning is incorporated along with spatial scanning. The middle lobe, which is effectively lost in the presence of its two larger neighbors, is still quite accurately reconstructed.

Next, we invert the same complex pit, but located now in an F-15 wing station, as shown in Figure 5. The coil, whose inner-radius is 0.25in, outer-radius 0.26in, height of 0.1in, has 10,000 turns, and is excited at 100Hz. We operate at this low frequency in order to penetrate the aluminum plates and get to the corrosion. The impedance response of the complex flaw at this frequency is shown in Figure 6. The result of the inversion is (0.028, 0.022, 0.033). The middle extreme is still sort of swallowed by the outer ones, but the indication of the profile in depth is still quite good, especially since the extreme value, 0.034, is well approximated by 0.033.

A Multifrequency Benchmark Inversion Test. In order to validate our inversion algorithm that utilizes NLSE, we performed a multifrequency experiment on a block of stainless steel that

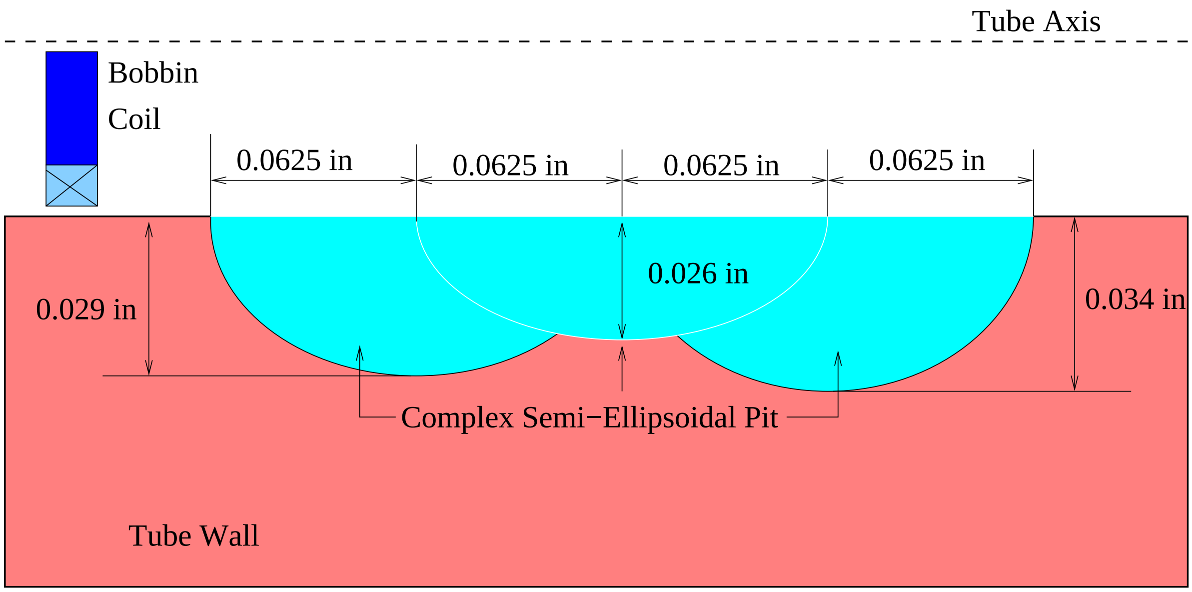

Figure 3: Illustrating a complex pit that comprises three intersecting semi-ellipsoids, whose dimensions are shown.

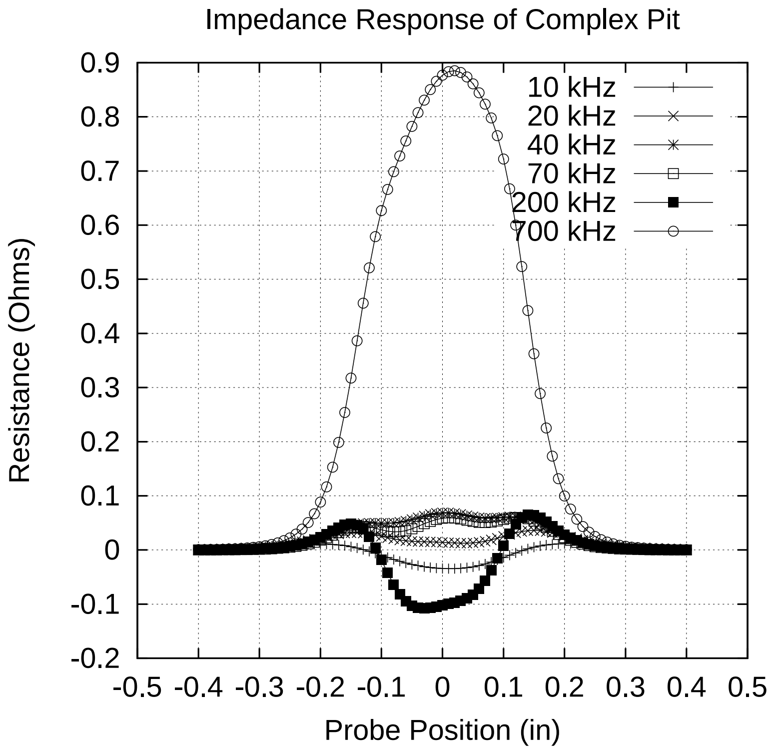

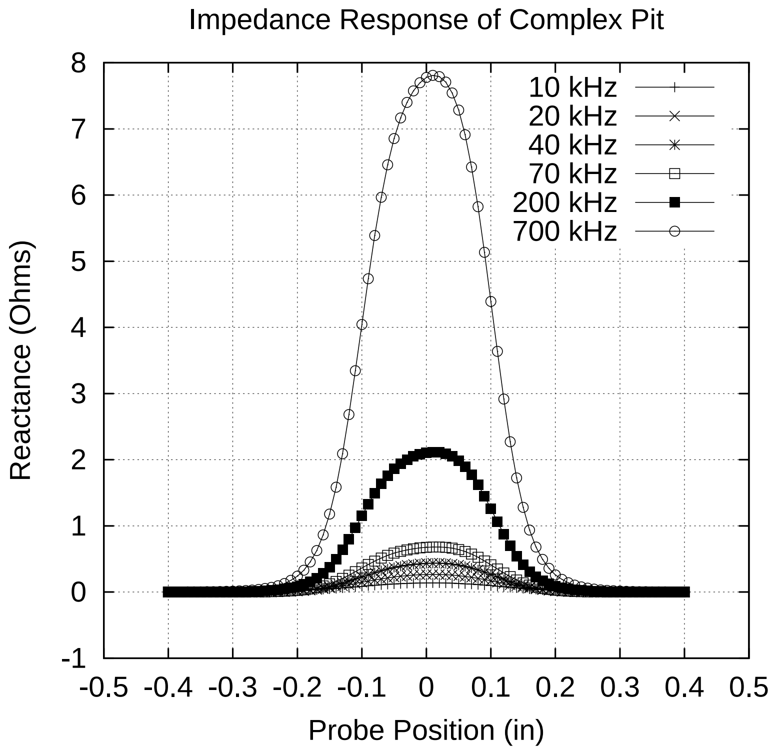

Figure 4: The model input impedance data to NLSE at 10kHz, 20kHz, 40kHz, 70kHz, 200kHz, and 700kHz: resistance (left), reactance (right).

Freq (kHz)	Result
10	(0.026, 0.022, 0.032)
20	(0.026, 0.023, 0.032)
40	(0.026, 0.023, 0.032)
70	(0.028, 0.023, 0.033)
200	(0.032, 0.026, 0.036)
700	(0.033, 0.030, 0.037)
Freq. Avg.	(0.029, 0.025, 0.034)
True	(0.029, 0.026, 0.034)

Table 2: Estimation of three C-axes for the complex semi-ellipsoidal pit model. The row labeled 'Freq. Avg.' is the average of the results over the six frequencies.

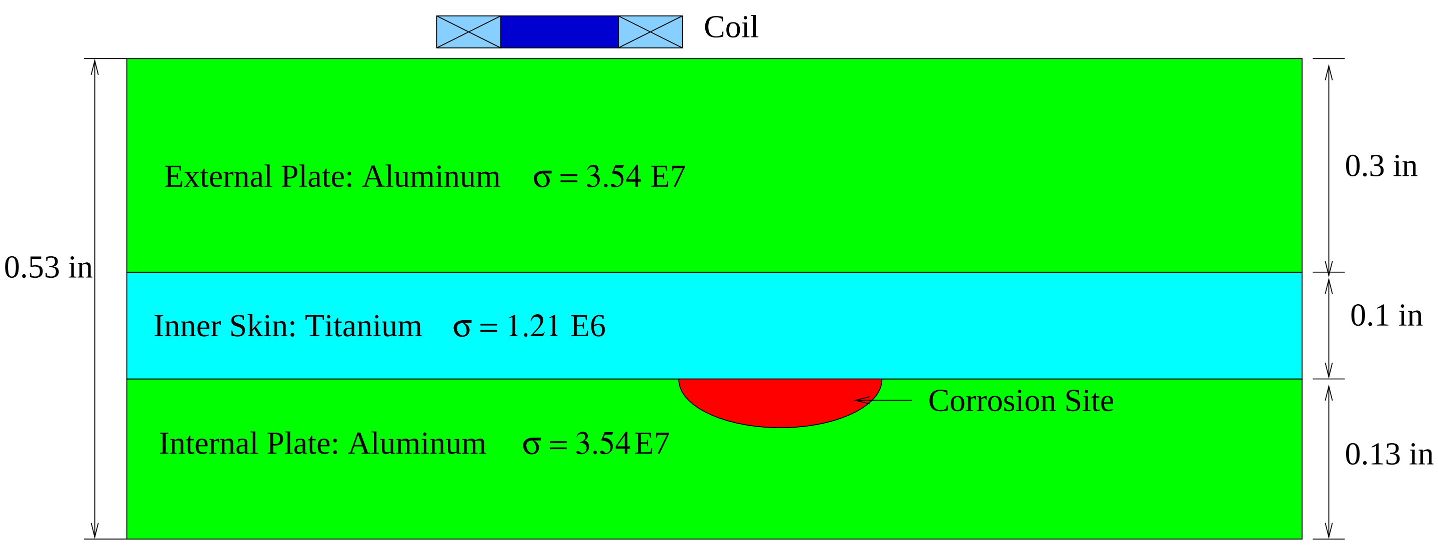

Figure 5: Inversion of a complex corrosion pit in an F-15 wing station.

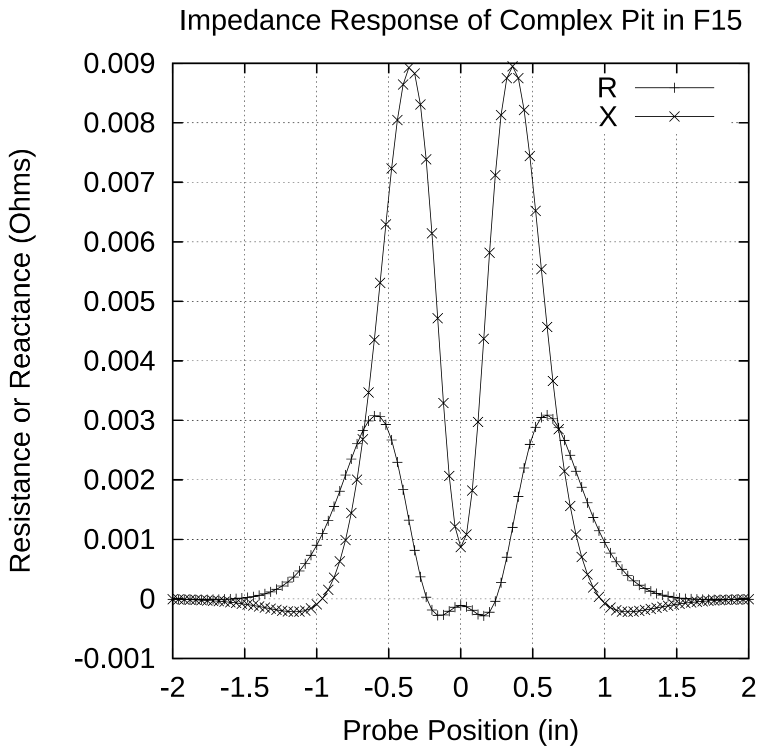

Figure 6: Input data for the inversion of a complex corrosion pit in an F-15 wing station.

contained a machined semi-ellipsoid, whose semi-axes were nominally 0.0625in $\times$ 0.0625 $\times$ 0.026in. Because we did not have the capability of scanning a coil over this defect, we simply laid the stainless-steel block over a coil that was embedded in an acryllic block, as in Figure 7, and then excited the coil over the frequency range of 0.1MHz to 1MHz, in 100kHz steps. The 'pit' was positioned as accurately as possible to be directly above the coil, whose dimensions were 15 mils inner radius, 48 mils outer radius, 7 mils height, and was wound with nineteen turns over two layers. The measured dc resistance of the coil was 0.741Ω, and the measured dc inductance was 0.51092μH.

The first task was to characterize the host material and to determine the lift-off of the coil over the host. This was done by taking multifrequency data when the coil is over the unflawed workpiece, and then introducing these data into NLSE. The results were that $\sigma_{\rm host} = 1.1763 \times 10^6$ S/m, lift-off=10.201 mils. These, then, are the 'host parameters' for the pit-inversion process.

The multifrequency input (impedance) data obtained when the pit is over the coil are shown in Figure 8, and these data are presented to NLSE in order to determine the X, Y- coordinates of the center of the coil from the center of the pit, as well as the values of the three semi-axes. The result of the inversion produced $X-$ and $Y-$coordinates of 6.711 mils and 6.695 mils, respectively, for the location of the probe from the center of the pit. The dimensions of the pit semi-axes were: A=0.0737in, B=0.0737in, C=0.0279in. The solution is least sensitive to the lateral coordinates of the probe relative to the pit, and most sensitive to the depth of the pit, as we noted before. This validates the NLSE inversion process, as it is applied to semi-ellipsoidal pit models.

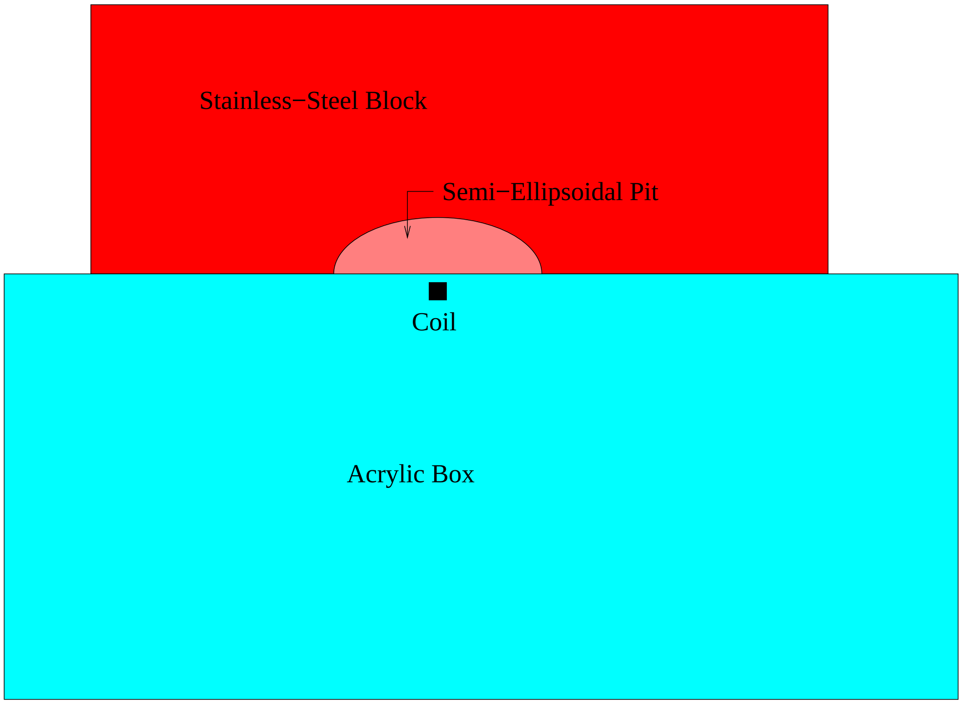

Figure 7: A multifrequency validation test. The coil is excited at 10 frequencies between 0.1MHz and 1.0MHz.

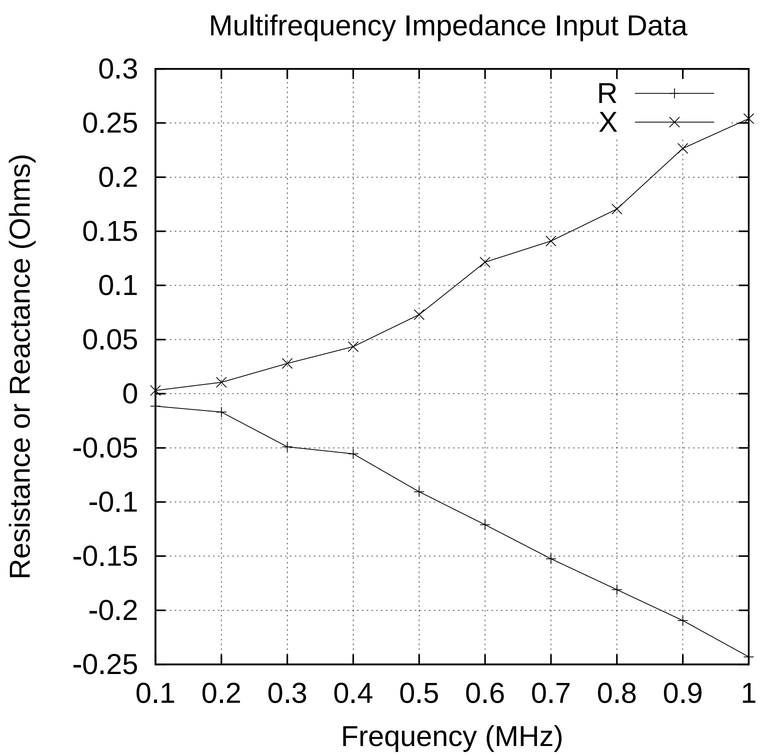

Figure 8: Multifrequency input data for the benchmark inversion test.